PROCEEDINGS of the
23rd International Congress on Acoustics

9 to 13 September 2019 in Aachen, Germany

Correction of Sound Pressure Levels Calculated for Small Rooms Using Diffuse-Field Theory

Kiyoshi MASUDA[1]; Hikari TANAKA[2]

[1] Taisei Corporation, Japan

[2] Taisei Corporation, Japan

ABSTRACT

The most frequently used method for predicting sound pressure levels arising in a room as a result of transmitted sound or floor impact sound from adjacent rooms is an acoustic energy calculation assuming a diffuse sound field. If the dimensions of the room under investigation are sufficiently large, pressure levels can be predicted accurately by this method. However, especially at low frequencies, the wavelength of the sound may exceed the room dimensions, leading to reduced predictive accuracy. Although the Waterhouse correction is typically used to correct for this error, its reliance on statistical energy considerations means that it cannot take into account the response to the frequency range lower than the first-order mode and to frequencies between adjacent lower-order modes. In this work, a new correction method is derived from the relationship between the sound pressure level calculated using wave theory and the sound pressure level using diffuse-field theory in the frequency range from lower than the first-order mode to a low-order mode. By comparing calculated results obtained using the new method with both actual measurements and FEM calculations, its accuracy is examined.

Keywords: Correction, Diffuse-Field Theory, Small Room, Wave theory, Prediction

1. INTRODUCTION

It is important to be able to predict sound pressure levels arising in a room as a result of transmitted sound or floor impact sound from adjacent rooms. This is typically done using an acoustic energy calculation in which a diffuse sound field is assumed. This method gives accurate results if the dimensions of the room under investigation are sufficiently large. However, in smaller rooms the wavelength of the sound may exceed the room dimensions, especially at low frequencies. This results in predictions of lower accuracy.

Two specific problems must be faced when applying the energy calculation to low frequencies. The first is the frequency characteristic of the amount of energy flowing into the sound field of the room. It occurs because certain phenomena cannot be taken into consideration in the energy calculation: resonance and antiresonance in the low-order mode of the sound field in the room, and periodic compression and rarefaction of air in the room at a frequency lower than the first-order mode frequency. The second problem is the deviation between the space-averaged squared sound pressure level of the entire room and that of the center area where measurement points are actually provided. It occurs because of the sound pressure distribution in the room. The energy calculation does not consider the distribution, because it assumes a diffuse sound field.

The Waterhouse correction [1] is typically used to correct for these problems [2]. This is a correction applied to the space-averaged squared sound pressure in a room as calculated by energy theory; it assumes that the energy density near the room boundary is higher than that near the center of the room. As a method of correcting the sound pressure at any arbitrary point away from the boundary of the room, it is unable to fundamentally solve the first of the above problems while its correction for the second problem may include a large error depending on the relationship between the size of the room and the wavelength.

The purpose of this research is to derive a correction that approximates the wave phenomenon

[1] kiyoshi.masuda@sakura.taisei.co.jp
[2] tnkhkr00@pub.taisei.co.jp

separately for both of the above-mentioned problems. The authors propose a method that can approximate the sound pressure level of a small room using diffuse sound field theory without the need to invoke wave theory calculations. The accuracy of the method is examined by comparing its calculation results with results of the wave theory calculations and laboratory experiments.

2. OUTLINE OF CORRECTION METHOD

A correction equation is defined as follows for approximating the space-averaged squared sound pressure level of the entire room of the actual wave field ($L_{p.wave}$) from the space-averaged squared sound pressure level obtained using the energy calculation based on diffuse sound field theory ($L_{p.ene}$).

$$L_{p.wave} \approx \tilde{L}_{p.wave} = L_{p.ene} + \Delta L_{sf} \tag{1}$$

Here, $\tilde{L}_{p.wave}$ is the approximated $L_{p.wave}$ and ΔL_{sf} is a correction factor for the frequency characteristic of the amount of energy flowing into the sound field of the room that accounts for resonance and anti-resonance, in the low-order mode and periodic compression and rarefaction of air in the room at a frequency lower than the first-order mode frequency.

In addition, taking into consideration that measurements are actually performed near the center of a room, another correction equation is defined for approximating the space-averaged squared sound pressure level of the sound field within a central volume defined by a fixed distance from the boundary of the room ($L_{p,area}$) from the space-averaged squared sound pressure level of the entire room of the actual sound field ($L_{p.wave}$) as follows.

$$L_{p,area} \approx \tilde{L}_{p,area} = \tilde{L}_{p.wave} - \Delta L_{mp} \tag{2}$$

Here, $\tilde{L}_{p,area}$ is the approximated $L_{p,area}$, and ΔL_{mp} is the correction value for the sound pressure distribution in the room.

Therefore, the full equation for correcting the energy calculation result obtained using diffuse sound field theory is as follows.

$$L_{p,area} \approx \tilde{L}_{p,area} = L_{p.ene} + \Delta L_{sf} - \Delta L_{mp} \tag{3}$$

The corrected value will then reflect actually measured sound pressure levels. In the sections that follow, the derivation of correction values ΔL_{sf} and ΔL_{mp} will be examined.

3. CORRECTION FOR LOW-ORDER MODE OF SOUND FIELD

3.1 Examination by One-Dimensional Sound Field

In order to explain in an easy-to-understand manner the characteristics of the discrepancies that occur between actual wave phenomenon and the diffuse sound field theory, we here consider a one-dimensional sound field and predict the sound pressure resulting from a floor impact as shown in Fig. 1. A ceiling with a sound absorption coefficient of zero vibrates at velocity v at all frequencies and emits sound. The sound is reflected at the floor which has sound absorption α at all frequencies. The sound pressure $p(x)$ at any point x can be calculated by the following equations:

$$p(x) = \rho c v \left[e^{-jkx} + \frac{(Z-1)e^{-jkH}}{(Z+1)e^{jkH}} e^{jkx} \right] \Bigg/ \left[1 - \frac{(Z-1)e^{-jkH}}{(Z+1)e^{jkH}} \right], \quad k = \frac{2\pi f}{c}, \alpha = \frac{4Z/\rho c}{(Z/\rho c + 1)^2} \tag{4}$$

Here, ρ is the density of air, c is the speed of sound, H is the ceiling height, Z is the floor impedance, and f is the frequency. $L_{p.wave}$ of the one-dimensional sound field is the space-averaged sound pressure level of the entire sound field calculated using Eq. (4). On the other hand, $L_{p.ene}$ of the one-dimensional sound field using the energy calculation not considering phase is given by Eq. (5).

$$L_{p.ene} = 10\log_{10}(\rho c v^2/\bar{\alpha}), \ \bar{\alpha} \approx \alpha/2 \tag{5}$$

Figure 2 shows the calculated results of $L_{p.wave}$ and $L_{p.ene}$ when the ceiling height H is 2,650 mm, the average sound absorption coefficient $\bar{\alpha}$ is 0.09, and the vibration velocity level of the slab is -120 dB re 1m/s. According to Fig. 2, $L_{p.ene}$ is calculated to be smaller than $L_{p.wave}$ at the mode frequency of the sound field, and larger than $L_{p.wave}$ at the antiresonance frequency. Also, at frequencies lower than the first-order mode, the lower the frequency, the smaller the difference between $L_{p.wave}$ and $L_{p.ene}$. If the frequency is sufficiently high in a three-dimensional sound field, and in the 1/3 octave band description, such a difference is considered to be almost eliminated, because the mode density rises rapidly. However, in small rooms, the same tendency is expected to occur at lower frequencies.

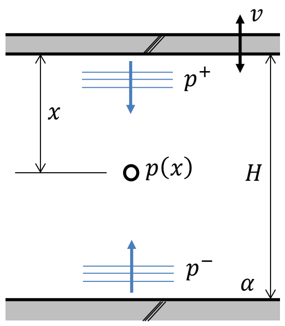

Figure 1 – Calculation model

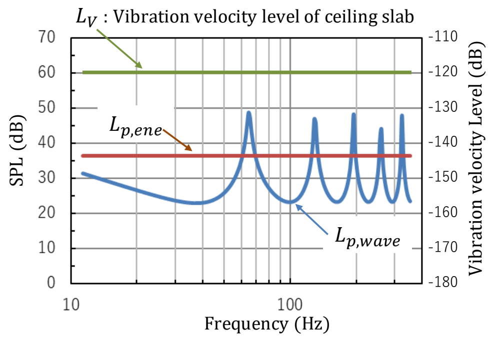

Figure 2 – Calculated results by wave and energy theory (H=2650mm)

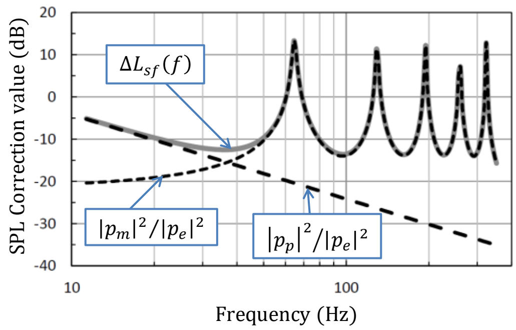

Figure 3 – Sound level correction curve

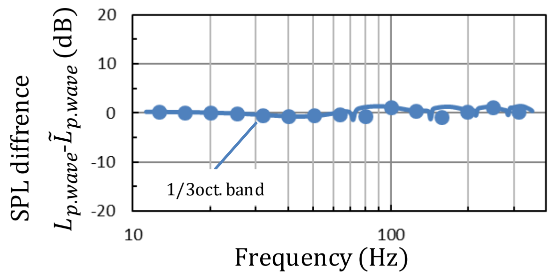

Figure 4 – Difference between wave and energy theory with correction

3.2 Correction Value ΔL_{sf} for One-Dimensional Sound Field

Here, a correction value ΔL_{sf} for the one-dimensional sound field that can approximate $L_{p.wave}$ from $L_{p.ene}$ without a wave theory calculation is derived.

The space-averaged squared sound pressure $|p_e|^2$ is the physical quantity of $L_{p.ene}$ normalized by the sound pressure p_{max} which is the the physical quantity of $L_{p.wave}$ at the m^{th}-order resonance frequency f_m and is approximated by the following equations:

$$|p_e|^2 = \frac{b}{f_1}\tan^{-1}\frac{2f_1}{b}, f_m = mc/2H, b = \frac{-c\log_e(1-\bar{\alpha})}{6.27 \times H} \tag{6}$$

On the other hand, the space average of the squared sound pressure $|p_m|^2$ is the physical quantity of $L_{p.wave}$ normalized by p_{max} and is approximated by the following equations:

$$|p_m|^2 = \sum_{m=1}^{\infty} [1 + 4|f - f_m|^2/b^2]^{-1} \tag{7}$$

Furthermore, the ratio of the space average of the squared sound pressure $|p_p|^2$ below the first-order mode frequency of $L_{p.wave}$ to $|p_e|^2$ is given by the following equation:

$$|p_p|^2/|p_e|^2 = c^2\bar{\alpha}/(2\pi f H)^2 \tag{8}$$

Therefore, the correction value ΔL_{sf} for a one-dimensional sound field is obtained as below.

$$\Delta L_{sf}(f) = 10\log_{10}\left[\frac{|p_m|^2}{|p_e|^2} + \frac{|p_p|^2}{|p_e|^2}\right] \tag{9}$$

The calculated values of ΔL_{sf}, $|p_m|^2/|p_e|^2$, and $|p_p|^2/|p_e|^2$ under calculation conditions identical to those in Fig. 2 are shown in Fig. 3. The calculated ΔL_{sf} is very similar to the difference between $L_{p.wave}$ and $L_{p.ene}$ in Fig. 2, so it can be considered an appropriate correction value.

The difference between $L_{p.wave}$ and $\tilde{L}_{p.wave}$ as calculated by Eqs. (5) to (9) is shown in Fig. 4. Here, the ceiling height H is 2,400 mm and the average sound absorption coefficient $\bar{\alpha}$ is 0.09. It can be seen that the difference is small in all frequency bands.

3.3 Examination by Three-Dimensional Sound Field

Frequency response analysis is performed using the finite element method (FEM), assuming that the room affected by the sound is under a vibrating ceiling concrete slab, as shown in Fig. 5. Three ceiling heights H are considered: 2,400 mm, 2,650 mm, and 2,800 mm. The ceiling slab is modeled using shell elements, while the sound field in the room is modeled with fluid elements. The boundary condition at the four edges of the ceiling slab is a simple support and the boundary conditions applied to wall and floor surfaces are an impedance condition where the absorption coefficient for normal incidence is 0.09.

A vibrational excitation force of 1 N in the vertical direction is input at the excitation point on the ceiling slab for each frequency, and the sound pressure at the nodal points of fluid elements and the vibration velocity of the nodal points of shell elements are calculated. The mean squared sound pressure level of all nodal points of fluid elements is taken as $L_{p.wave}$.

$L_{p.ene}$ is calculated using Eq. (10).

$$L_{p.ene} = \bar{L}_V + 10\log_{10}\frac{4S_{eff}\sigma\rho^2c^2}{S_a\bar{\alpha}p_0^2} \tag{10}$$

Here, $\bar{L}_V$ is the surface-averaged squared vibration velocity level of all nodal points of shell elements in the sound radiation area. S_{eff} is the radiation area of the ceiling slab, σ is the acoustic radiation efficiency of the ceiling slab (set to 1.0), S_a is the surface area of the room affected by the sound, and p_0 is the reference sound pressure ($p_0 = 2\times10^{-5}$ [Pa]). The calculated results of $L_{p.wave}$, $L_{p.ene}$ and $\bar{L}_V$ for the 2,650 mm ceiling height are shown in Fig. 6. In addition, the difference between $L_{p.wave}$ and $L_{p.ene}$ is shown in Fig. 7 for all three ceiling heights.

The frequency dependence of the $L_{p.wave}$ and $L_{p.ene}$ difference is more complicated than in the one-dimensional sound field. However, in the frequency range below the vertical first-order mode frequency, the frequency characteristics are very similar to those in the one-dimensional sound field. The reason for this seems to be that the vertical vibration mode is more easily excited than the horizontal vibration mode because the slab occupies only the horizontal plane and the mode density is low. At higher frequencies, the number of modes rapidly increases, so that it is close to the diffuse sound field, and the deviation itself becomes smaller.

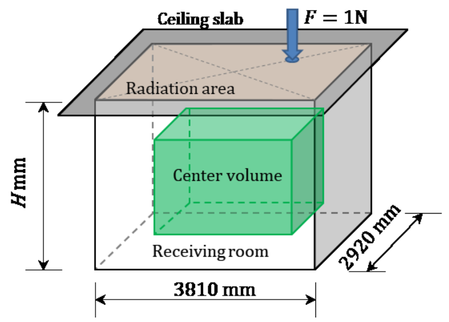

Figure 5 – Calculation model for FEM

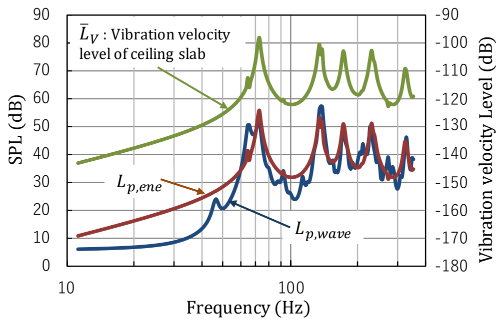

Figure 6 – Calculated results by wave and energy theory (H=2650mm)

3.4 Correction Value ΔL_{sf} for Three-Dimensional Sound Field

As shown above, the difference between $L_{p.wave}$ and $L_{p.ene}$ in the three-dimensional sound field is very similar that in the one-dimensional sound field up to around the frequency of the first-order mode in the vertical direction. Therefore, the correction ΔL_{sf} for one-dimensional sound field is modified for the three-dimensional case as follows.

First, the space average of the squared sound pressure $|p_m|^2$ is assumed to be as given by Eq. (7) up to the second-order mode. Then the influence of rapidly increasing higher modes is approximated by adding a large sound absorption coefficient in the second-order mode. Equation (7) is thus modified to obtain the following equation:

$$\frac{|p_m|^2}{|p_e|^2} = \begin{cases} \displaystyle\sum_{m=1}^{2} \left[1 + 4|f - f_m|^2/{b_m}^2\right]^{-1} \left[\frac{1}{f_1}\tan^{-1}\frac{2f_1}{b_m}\right]^{-1}, & f < f_2 \\ max\left(\displaystyle\sum_{m=1}^{2} \left[1 + 4|f - f_m|^2/{b_m}^2\right]^{-1} \left[\frac{1}{f_1}\tan^{-1}\frac{2f_1}{b_m}\right]^{-1}, 1\right) & f \geq f_2 \end{cases} \tag{11}$$

$$b_m = \frac{-c\log_e(1 - \bar{\alpha}_m)}{6.27 \times H}$$

Here, $\bar{\alpha}_m$ is the sound absorption coefficient at the frequency of the m^{th}-order mode in the vertical direction. Equation (8) is then modified to obtain the following equation to fit the three-dimensional sound field:

$$\frac{|p_p|^2}{|p_e|^2} = \frac{S_a c^2 \bar{\alpha}}{4S_{eff}(2\pi f H)^2} \tag{12}$$

The values of ΔL_{sf}, $|p_m|^2/|p_e|^2$, and $|p_p|^2/|p_e|^2$ for Fig. 5 calculated using Eq. (11) and Eq. (12) are shown in Fig. 8. Here, the height of the ceiling is 2,650 mm and the average sound absorption coefficient is 0.073 for the first mode and 0.7 for the second mode.

The difference between $L_{p.wave}$ calculated using FEM and $\tilde{L}_{p.wave}$ calculated using Eqs. (1), (9), (10), (11) and (12) is shown in Fig. 9. In this three-dimensional calculation, it can be seen that the wave calculation result is well approximated only with the addition of the correction value ΔL_{sf} to the energy calculation result $L_{p.ene}$.

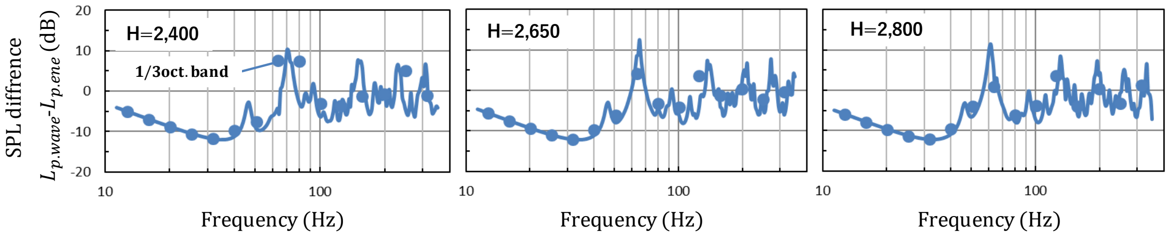

Figure 7 – Difference between wave and energy theory (3D)

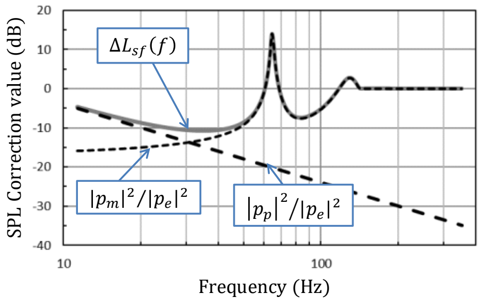

Figure 8 – Sound level correction curve

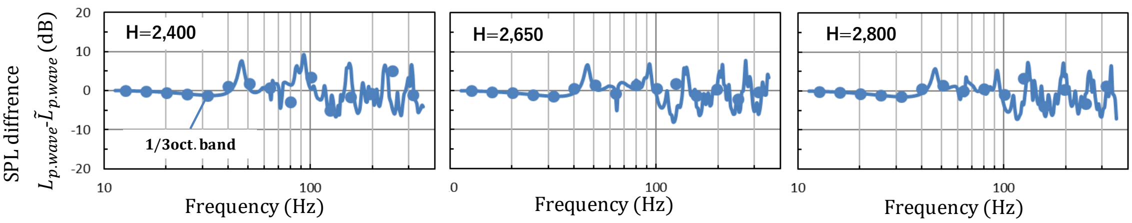

Figure 9 – Difference between wave and energy theory with correction

3.5 Laboratory Experiment on ΔL_{sf}

In the laboratory outlined in Fig. 10, an excitation point (V3) on the ceiling concrete slab is excited with a constant force. The vibration velocity level of the slab and the sound pressure level in the room are measured at large numbers on grid points (on a pitch of approximately 280 mm).

$L_{p.wave}$ is the space-averaged squared sound pressure level of all measurement points in the room's sound field. $L_{p.ene}$ is calculated using Eq. (10). $\bar{L}_V$ is the surface-averaged squared vibration velocity level of all measurement points on the ceiling slab. The correction value ΔL_{sf} is calculated using Eqs. (9), (11) and (12), where $\bar{\alpha}_1$ is 0.3 and $\bar{\alpha}_2$ is 0.7.

The difference between measured $L_{p.wave}$ and approximated $\tilde{L}_{p.wave}$ calculated using Eqs. (1), (9), (10), (11) and (12) is shown in Fig. 11, and the difference between $L_{p.wave}$ and $\tilde{L}_{p.wave}$ is shown in Fig. 12. An improvement is seen in the 1/3 octave band, especially below 100 Hz.

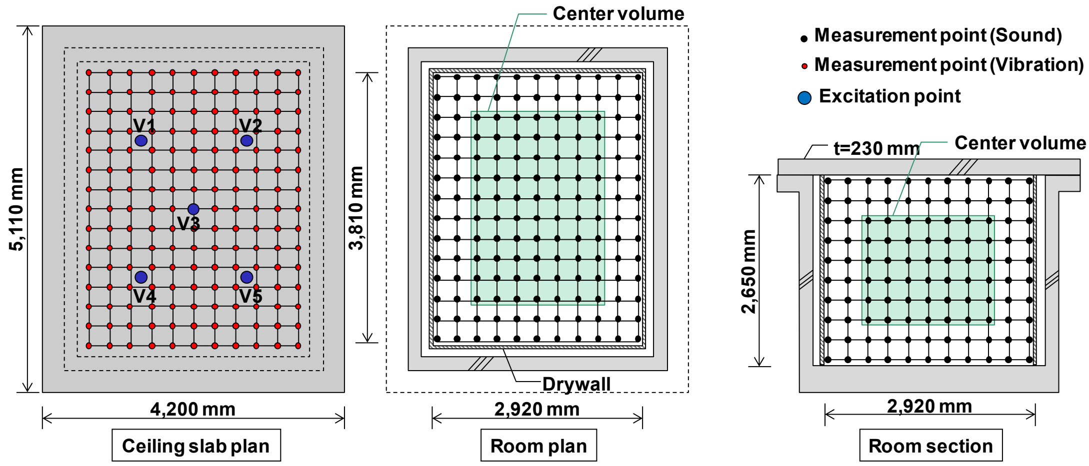

Figure 10 – Experimental condition

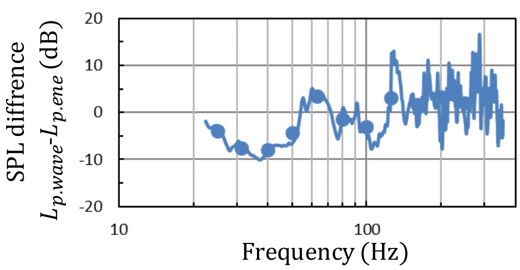

Figure 11 – Difference between measurement and energy calculation

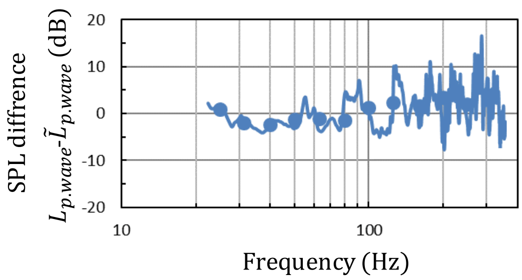

Figure 12 – Difference between measurement and energy calculation with correction

4. CORRECTION FOR SOUND PRESSURE DISTRIBUTION

4.1 Examination by One-Dimensional Sound Field

The variation in sound pressure distribution with frequency in the one-dimensional sound field is shown in Fig. 13. At frequencies lower than the first-order mode (A), the sound pressure in the sound field is constant everywhere, as in the inner space of an air spring. At the frequency of the first-order mode (B), the sound pressure increases at the boundary and decreases in the center volume of the sound field.

Therefore, in frequency range (A), since there is almost no variation over the entire sound field, it can be considered that there is almost no difference between the average value in the center volume and the average value of the entire sound field. However, at mode frequencies such as (B), the lower the mode, the larger the difference between the average value in the center volume and the average value of the entire sound field.

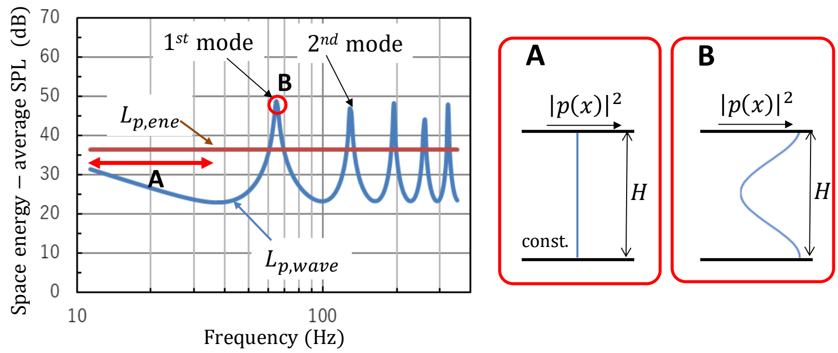

Figure 13 –Squared sound pressure distribution in one-dimensional sound field

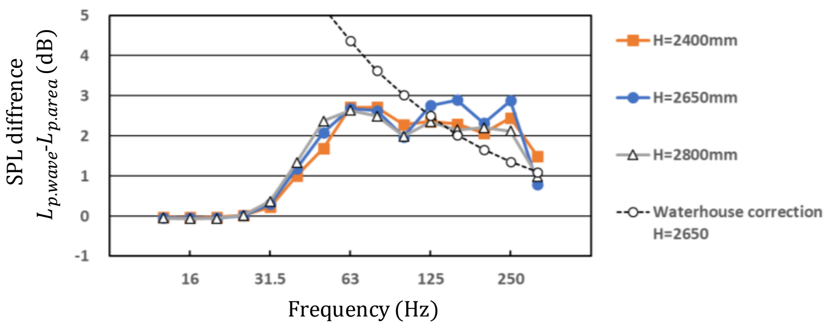

Figure 14 – Difference between $L_{p.wave}$ and $L_{p,area}$

4.2 Examination by Three-Dimensional Sound Field

In the FEM calculation model shown in Fig. 5, the mean squared sound pressure level of only the nodal points in the center volume 500 mm away from the ceiling, wall and floor respectively is taken as $L_{p,area}$. The difference between $L_{p.wave}$ and $L_{p,area}$ is shown in Fig. 14. Here the three ceiling heights of 2,400 mm, 2,650 mm and 2,800 mm are considered as before. The value of the Waterhouse correction at $H =$ 2,650 mm is also shown for reference.

The Waterhouse correction takes a larger value as the frequency decreases, but the calculated difference starts to decrease near the first-order modal frequency in the vertical direction, and below 31.5 Hz becomes almost zero. The frequency range below 31.5 Hz corresponds to frequency range (A) in Fig. 13.

4.3 Correction Value ΔL_{mp} for Three-Dimensional Sound Field

Based on the discussion that follows, correction values for the sound pressure distribution ΔL_{mp} are defined as the following equations:

$$\Delta L_{mp} = \begin{cases} 0 & f < f_1/2 \\ 10\log_{10}(2f/f_1) & f_1/2 \le f < f_1 \\ min\left(3, 10\log_{10}(1 + S\lambda/8V + L\lambda^2/32\pi V)\right) & f \ge f_1 \end{cases} \tag{13}$$

First, based on the above results, set $f_1/2$ as the frequency at which the influence of the pressure field is large, and then increase by 1 dB every 1/3 octave from that point up to the frequency of the first-order mode. Above the first-order mode frequency, the correction basically follows the Waterhouse rule, but a maximum value is set at 3 dB. In equation (13), S is the surface area of the room, λ is the wavelength, V is the volume of the room, and L is the entire perimeter of the room.

The calculation results of ΔL_{mp} for $H =$ 2,400 mm in Fig. 5 and the difference between $L_{p.wave}$ and $L_{p,area}$ are shown in Fig. 15. It can be seen that the correction value closely approximates the sound pressure distribution in the room.

4.4 Laboratory Experiment on ΔL_{mp}

In the laboratory results shown in Fig.10, the mean squared sound pressure level at only the measurement points in the center volume 500 mm away from the ceiling, wall and floor respectively is taken as $L_{p,area}$. Calculated ΔL_{mp} values for the laboratory measurements and the difference between $L_{p.wave}$ and $L_{p,area}$ are shown in Fig. 16. In the frequency range below 80 Hz, the correspondence between ΔL_{mp} and the measured difference is very good. At 100 Hz or more, the correction value ΔL_{mp} is rather smaller, but the difference is at most about 1.5 dB, so accuracy is sufficient as a correction value.

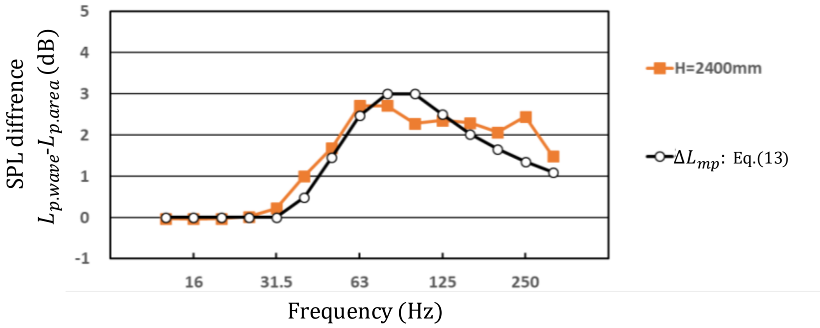

Figure 15 – Correction value and difference between $L_{p.wave}$ and $L_{p,area}$

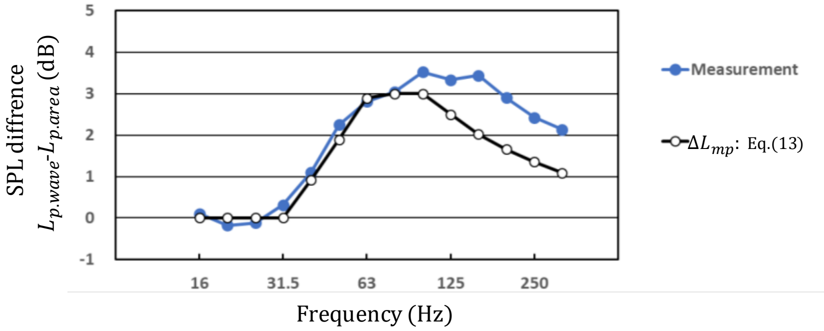

Figure 16– Actual difference between entire room average and center volume average in real room

5. CONCLUSIONS

A small-room correction method is proposed for the conventional diffuse sound field energy calculation, in which it is assumed that frequencies are low. The proposed correction includes two terms. One is for the influence of low order modes and periodic compression and rarefaction of air in the room at a frequency lower than the first-order mode frequency, and the other is for the influence of sound pressure distribution. The correction method well approximates the space-averaged square sound pressure level in simulated and measured sound fields without the need to invoke wave theory calculations.

Future work is to examine the correspondence between the correction and measurements in more sound fields with the aim of making the correction method more accurate.

REFERENCES

1. Waterhouse, R. V., “Interference patterns in reverberant sound fields.,” J. Acoust.Soc. Am., 1955.
2. ISO 12354-1:2017, Building acoustics – Estimation of performance of buildings from the performance of elements – Part 1: Airborne sound insulation between rooms